Project information

Project full title	European network for developing new horizons for RIs
Project acronym	EURIZON
Grant agreement no.	871072
Instrument	Research and Innovation Action (RIA)
Duration	01/02/2020 – 31/01/2024
Website	https://www.eurizon-project.eu/

Deliverable information

Deliverable no.	D4.19 (M46)
Deliverable title	Study report on a compact 6GeV high-brightness Linac (C-band) for top-up injection in storage rings and FEL applications
Deliverable responsible	INFN
Related Workpackage/Task	WP4 / Task 4.4
Type (*e. g.* Report; other)	Report
Author(s)	A. Giribono, F. Pannek, G. Geloni, S. Molodtsov, C. Vaccarezza
Dissemination level	Public
Document Version	1
Date	31 January 2024 (month 48)
Download page	https://www.eurizon-project.eu/

Document information

Version no.	Date	Author(s)	Comment
1	31 January 2024	A. Giribono, F. Pannek, G. Geloni, S. Molodtsov, C. Vaccarezza	–

Contents

Study report on a compact 6GeV high-brightness Linac (C-band) for top-up injection in storage rings and FEL applications

1 Introduction

In this deliverable we report the study results for a 6 GeV accelerator defined in the framework of Task 4.4 useful as injector for high brightness soft Free Electron Laser X-ray and for storage rings (namely the top-up injection). The machine layout foresees a 6 GeV linac equipped with an RF photogun for driving the FEL by means of a high-brightness electron beam and a thermionic gun for the top-up injection scheme into the storage ring. A similar injection scheme has been adopted also for SuperKEK-B and MAX-IV and is proposed for FCC-ee, even if in this case the two sources, RF photo and thermionic gun, are meant to share the same booster linac provided the injection of the second beam, for example the hight brigthness one, coming from a parallel Photoinjector operating with the emittance compensation scheme, at the energy of around 120 MeV, where a sufficient electron beam rigidity is granted. Since the study of the thermionic gun and top-up linac operation has already been completed and previously reported, the scheme of the 6 GeV FEL radiation source is here described based on the C-band technology option, that allows the reduction of the overall length of the Linac, as designed for Task 4.4 driven by a high brightness 250 pC electron beam with a final energy of 6 GeV.

2 S-band linac as injector for the storage ring

The first option of the full S-band injector for the storage ring was based on an RF thermionic gun followed by 86 Standing Wave Biperiodical Accelerating Structures (BAS) [1, 2]. The description of the S-band injector useful for the storage ring is not object of this report since it is well documented in literature [3]. This type of linac can produce 250 mA electron beam with the features reported in Table 1. In order to reduce the overall length of the accelerator an upgrade to higher frequencies was foreseen based on INFN expertise in designing and producing C-band SW and TW accelerating structures up to 2 m length, and a Linac based on C-band technology is discussed and described in the following sections.

Table 1: Electron beam parameters at the exit of the S-band top-up injector

E	6.0	GeV
$\epsilon_{x,y}$	1.5	nm-mrad
Bunch length	25-34	ps
Energy spread	0.20-0.35	%
Current transmission coefficient	46.5	%

3 C-band linac for FEL applications

The C-band linac for the FEL applications relies on a Standing Wave RF photogun followed by a Traveling Wave RF linac to boost the beam energy. The beamline is designed to produce high brightness beams to produce fel radiation with wavelength in the nm scale. In details, the nominal working point of the machine foresees a 250 pC beam with 6 GeV energy, up to 5 kA peak current, less than 0.6 mm-mrad slice emittance and less than 2 MeV slice energy spread.

The linac is based on the combination of an high brightness photoinjector and an high gradient booster linac. The photoinjector, where the beam explores the collective effects at very low energy, is set to maximise the transverse beam quality. The high-gradient booster linac allows for few GeV electron beams in a relatively small footprint accelerator, preserving the transverse beam quality and improving the ultimate 6D beam quality thanks to the insertion of two magnetic longitudinal compressors. A laser heater is also inserted to mitigate the microbunching instability that arises because of high longitudinal compression factors. The linac layout is reported in Figure 2.

The proposed C-band photo-injector, designed and simulated at Frascati National Laboratory (LNF), is the result of a long design study carried out in the framework of the CompactLight [4–6], EuPRAXIA@SPARC_LAB [7, 8] and IFAST projects [9]. It consists of a 2.6 cell standing wave (SW) gun, equipped with an emittance compensation solenoid,
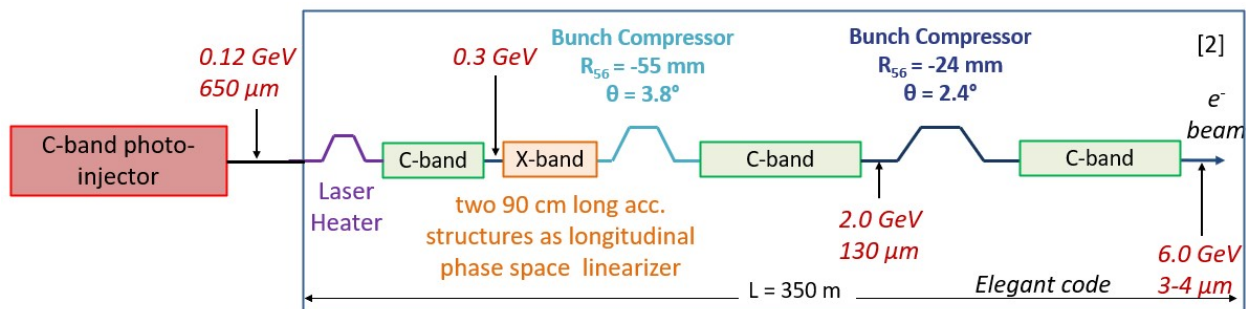
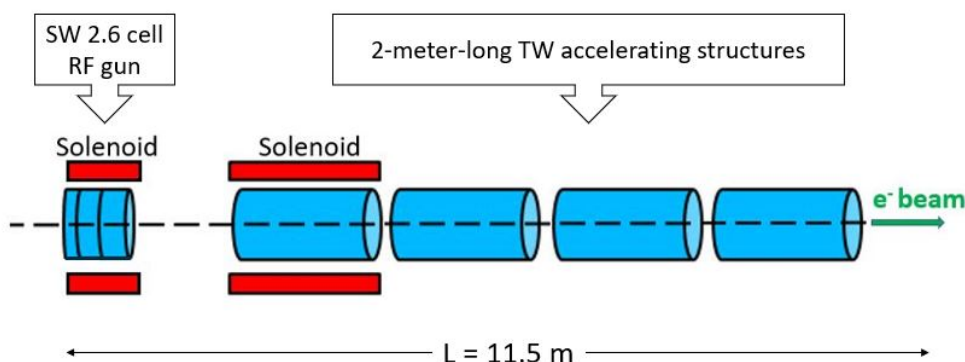Figure 1: Layout of the 6 GeV C-band linac.

Figure 2: The C-band photo-injector layout, designed and simulated at Frascati National Laboratory (LNF). It consists of a 2.6 cell standing wave gun, with an emittance compensation solenoid, followed by four travelling wave accelerating structures. The TW accelerating structures are two meter long and can be powered up to 31 MV/m (at 100 Hz repetition rate); the first one is surrounded by a solenoid.

followed by four travelling wave (TW) accelerating structures. The C-band TW accelerating structures are two meter long and can be powered up to 31 MV/m (at 100 Hz repetition rate); the first one is surrounded by a solenoid. A detailed description is reported in [10]

The C-band technology has been chosen for the photoinjector being a good compromise between the S and the X-band technology. It enables higher available peak field in the gun region, that results in beam brightness, and higher accelerating gradient in the TW accelerating structures if compared to the S-band technology; in the meanwhile it allows larger flexibility as regards the electron beam charge and length if compared to the X-band solution. In addition it should ensure a reliable operation at up to 1 kHz repetition rate.

The C-band linac design is inspired by the Swiss FEL machine layout as described in the conceptual design report [11]. It consists in three TW main linac to boost the beam energy, a laser heater at 150 MeV, two X-band 90 cm long accelerating structures to linearize the beam longitudinal phase space and two magnetic chicane to longitudinally compress the beam down to 3 μm.

4 Beam dynamics Studies

The beam dynamics has been studied by means of simulations with the ASTRA code [12] in the photoinjector at very low energy (space charge dominated regime) and with the Elegant code [13] along the booster linac (emittance-dominated regime).

4.1 The photoinjector

The photoinjector is set according to the invariant envelope theory [14] to enable the transverse emittance compensation, while the photo-cathode laser pulse at the cathode shows a cigar shape, i.e. flat-top longitudinal profile of 8.5 ps and uniform transverse distribution of about 0.17 mm, so to reduce the emittance degradation due to the transverse space charge forces before the beam becomes ultra-relativistic. The photoinjector is then set on-crest to obtain as much as possible low transverse emittance at the downstream booster entrance. Results of simulations are reported
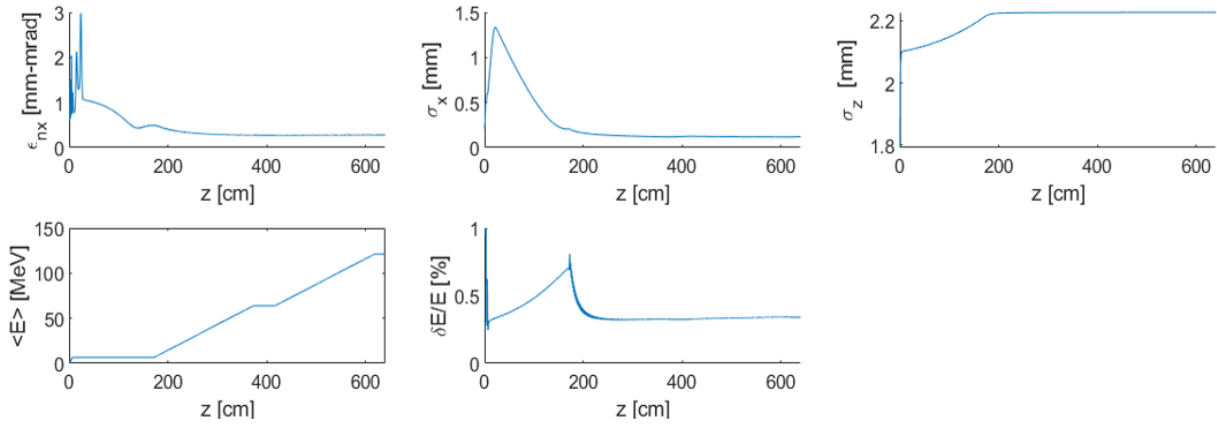
in Figures 3, 4 and Table 2.

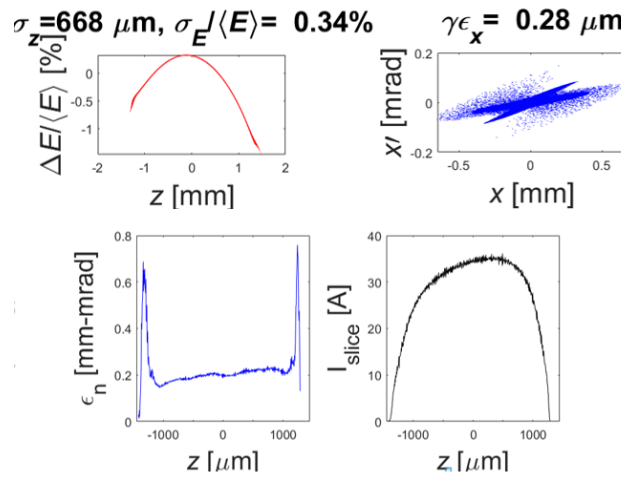Figure 3: Evolution of RMS beam parameters along the photoinjector

Figure 4: Electron beam phase space (top) and slice analysis (bottom) at the photoinjector exit

Table 2: Electron beam parameters at the photoinjector exit (250 pC)

E	0.122	GeV
$\epsilon_{nx,y}$	0.28	mm-mrad
Bunch length	670	μm
Energy spread	0.34	%
Peak current	35	A

4.2 The booster linac

The booster linac has been simulated with the Elegant code considering longitudinal space charge, Coherent Syncrotron radiation (CSR) and wakefields. It is operated off-crest to set the desired energy spread at chicane entrances, respectively 1 % and 0.4%, in the first two linac sections and to minimize the final beam energy spread at the last one. By means of matching quadrupoles and steering magnets the beam is carried at the FEL entrance and properly matched at the laser heater location and at the two magnetic chicanes entrance to avoid the emittance dilution due to the CSR. Whitin this machine the beam is boosted in energy and longitudinally compressed to obtain a 5kA peak current, less than 0.6 mm-mrad slice emittance and less than 2 MeV slice energy spread (<0.04%).

The Twiss parameters and the emittance behaviour along the linac are reported in Figures 5, 6.

Results of simulations are reported in Figures 7, 8 and Table 3. The Figure 7 reports the beam phase space and the slice analysis for the beam at the exit of the 6 GeV linac with the leaser heater switched-on; the Figures 7 reports the
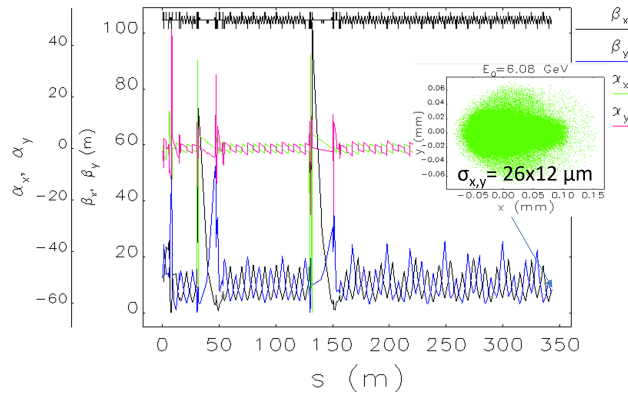
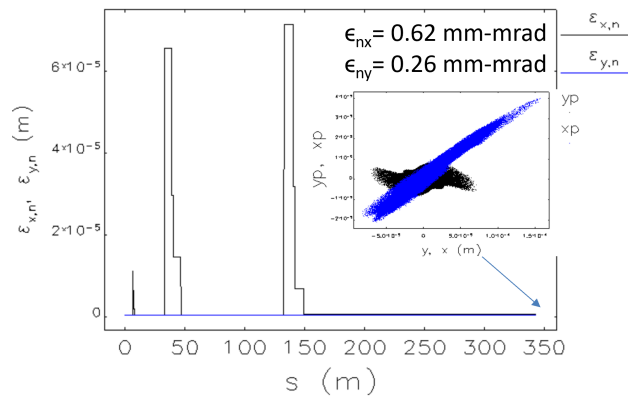Figure 5: Twiss function along the C-band booster linac

Figure 6: Transverse emittance along the C-band booster linac

effect of the laser heater that reduces the microbunching instability enabling a satisfying power value for the emitted fel radiation as discussed in the following.
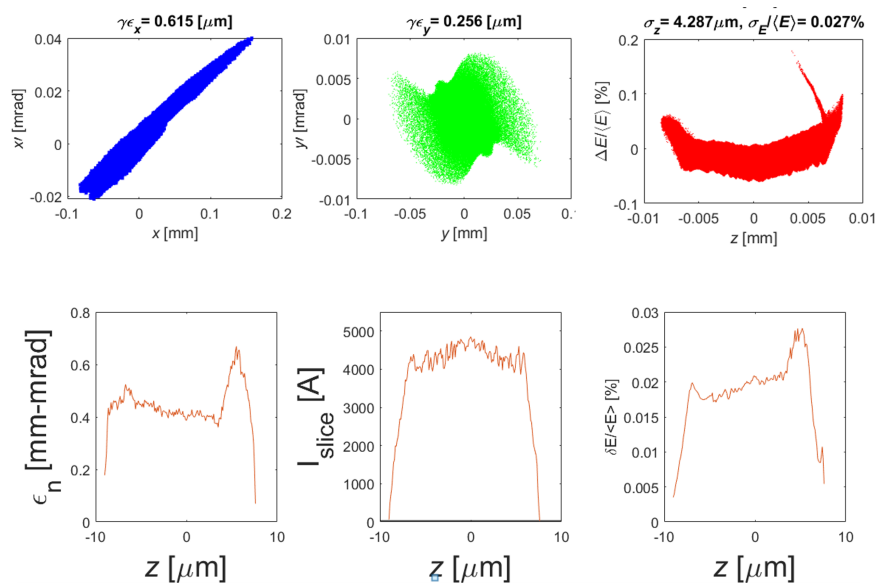

Figure 7: Beam phase space (top) and slice analysis (bottom) for the beam at the exit of the 6 GeV linac with the leaser heater switched-on.
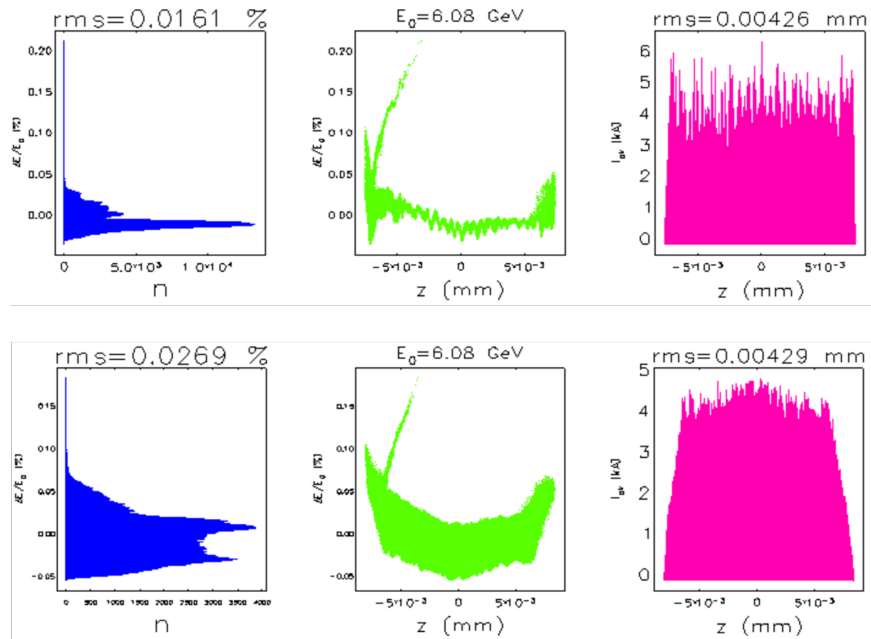
Figure 8: Longitudinal phase space analysis at 6 GeV with the laser heater switched off (top) and on (bottom).

Table 3: Electron beam parameters at the photoinjector exit (250 pC)

E	6.08	GeV
$\epsilon_{nx,y}$	0.62x0.26	mm-mrad
Bunch length	4.3	μm
Energy spread	0.027	%
Peak current	5	kA

5 The FEL radiation

5.1 The Undulator

In a first step, the FEL performance in the wavelength range from 1nm to 25nm is estimated by means of the analytical Ming Xie formalism [15] under consideration of a planar undulator. Here, also technical constraints regarding the maximum attainable magnetic field at a given undulator period length are taken into account on the example of a Nd-Fe-B hybrid Fe undulator with 8mm gap. Analysis shows that an undulator period length of 13cm offers a good compromise between gain length and saturation power, ranging from Lg=3.1m, Psat=70GW at 1nm to Lg=1.4m, Psat=110GW at 25nm, see Figure 9.

The FEL beamline lattice used for simulations with the FEL code Genesis 1.3 [16], v4 consists of 2.08 m long undulator segments (16 periods), with 0.42 m of space between each segment for beamline elements such as quadrupoles or diagnostics. The segment length is in the order of one power gain length to enable simple numerical tapering studies. Even though saturation is expected around 70m of beamline for the shortest FEL radiation wavelength of 1nm, a total of 50 undulator segments are used in the simulations to investigate the possibilities of post-saturation tapering (adjustment of the undulator magnetic field to compensate for the electron energy loss along the FEL undulator beamline).

5.2 Simulation results

The start-to-end simulations make use of a laser heated electron beam distribution to avoid detrimental effects due to the microbunching instability. The key beam parameters of the electron beam coming from the Linac and injected in the undulator are shown in the Figure 10, where energy, energy spread, current and transverse emittance are reported as function opf the longitudinal coordinate along the bunch (bunch tail at s=0).

The performance of the FEL driven by this beam is illustrated in the Figures 11-14 where, for the selected wavelength,s peak power and pulse energy evolution of the radiation are reported along the undulator position (above), together with the power spectrum and the normalized intensity of the pulse (below); no undulator tapering is applied here. For each case, 25 shots with different electron shot noise are simulated.
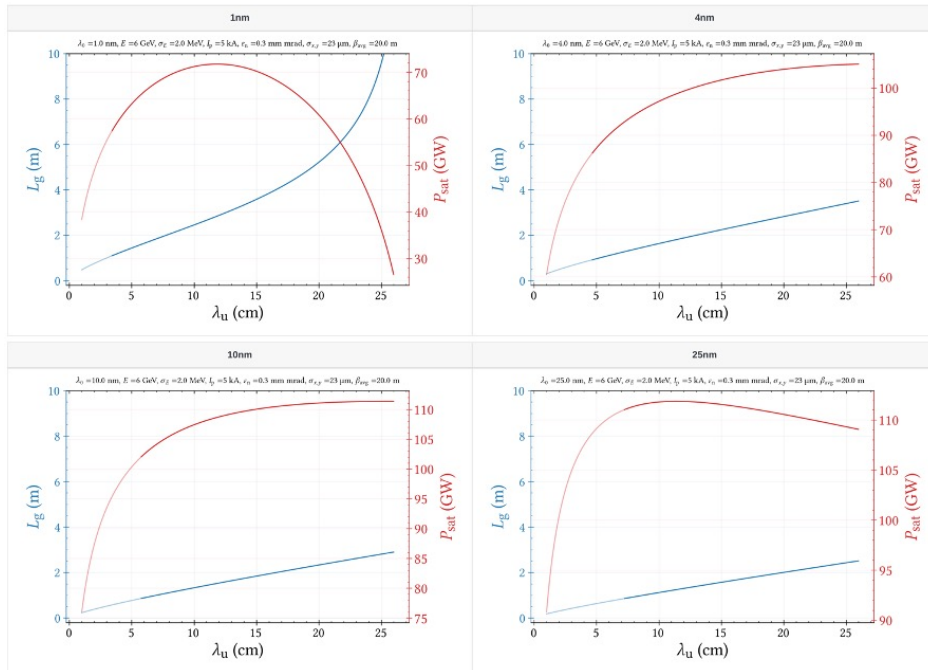
Figure 9: Undulator gain length and saturation power as function of the undulator period for 1-4-10-25 nm radiation wavelength (from right above in clockwise direction).
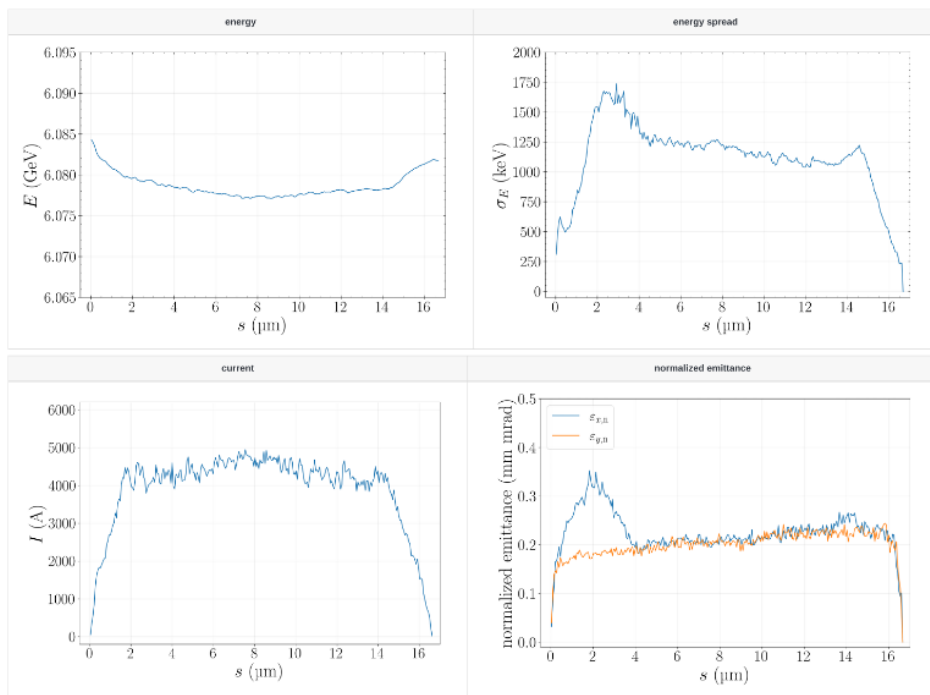

Figure 10: Slice analysis of the energy, energy spread, current and transverse emittance of the electron beam as coming form the tracking trough the C-band Linac.

The obtained results can be summarized as follows: The undulator tapering has been also considered for the 4nm case, to maximize the FEL power output. The results shown in 15indicate an increase in power and pulse energy by a factor of 2, and suggest a similar increase for the other presented wavelengths, although not forgetting tha ideal beam distribution taken into account.
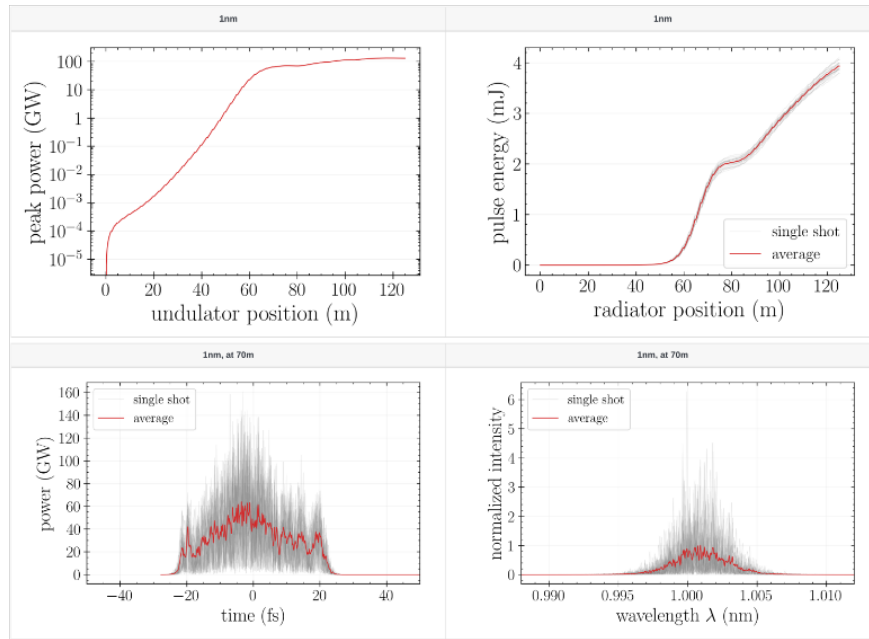
Figure 11: Peak power and pulse energy evolution of the 1 nm radiation vs the undulator position (above). Power spectrum and normalized intensity of the pulse (below).
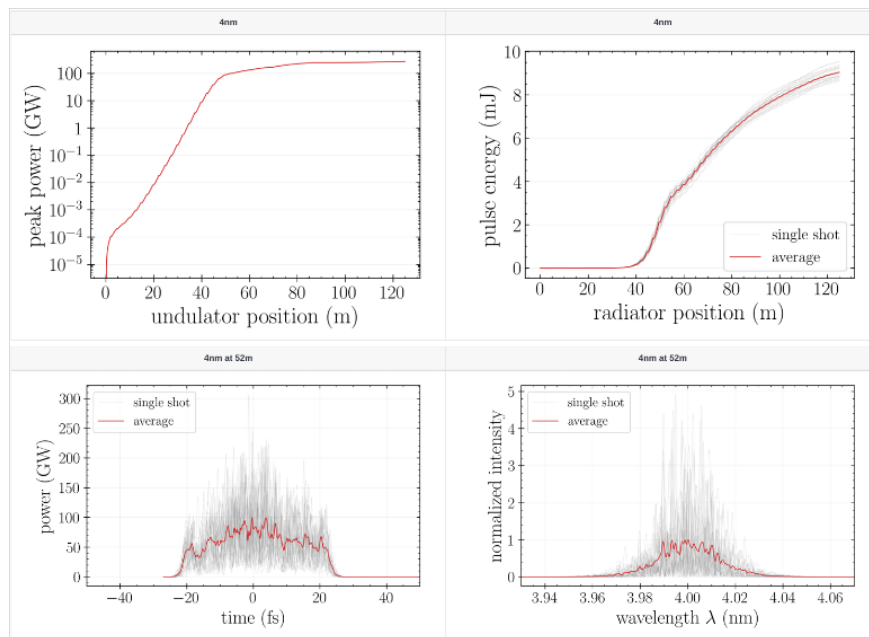

Figure 12: Peak power and pulse energy evolution of the 4 nm radiation vs the undulator position (above). Power spectrum and normalized intensity of the pulse (below).

Table 4: Undulator performance at the selected radiation wavelengths, without tapering

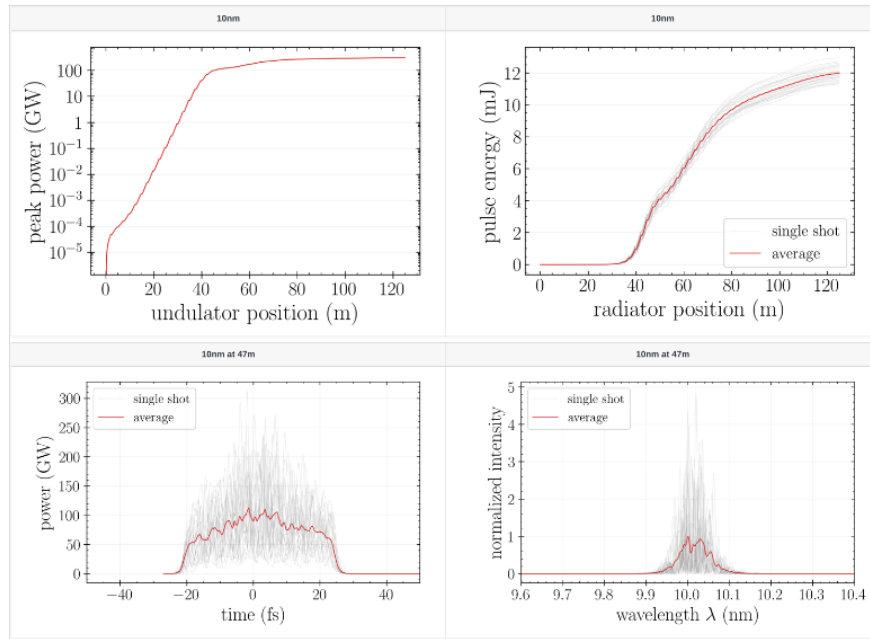| Wavelength (nm)	Saturation Power (GW)	Undulator length (m)
1	70	70
4	100	52
10	100	47
25	100	42

Figure 13: Peak power and pulse energy evolution of the 10 nm radiation vs the undulator position (above). Power spectrum and normalized intensity of the pulse (below).
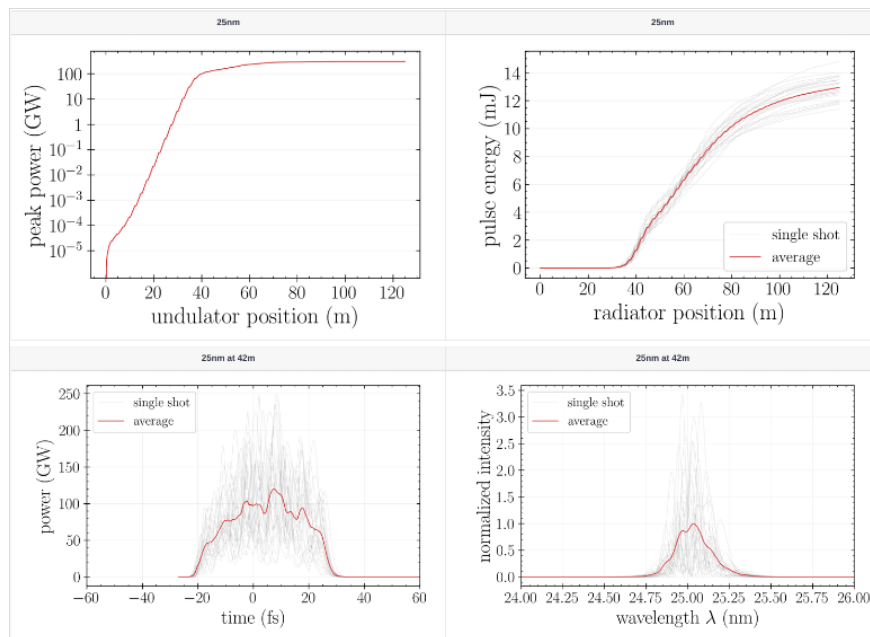

Figure 14: Peak power and pulse energy evolution of the 25 nm radiation vs the undulator position (above). Power spectrum and normalized intensity of the pulse (below).

6 Concluding & remarks

The Eurizon collaboration has finalized a proposal for a 6 GeV injector useful for top-up injection in a 6 GeV Synchrotron Ring and for driving a high brightness soft X-ray Free Electron Laser. Two electron beam sources have been studied such as RF thermionic gun for the injection into the storage ring and RF photogun for the injection into the FEL. Since the study of the thermionic gun and S-band top-up linac has already been completed and previously reported, a 6 GeV FEL radiation source is here presented for Task 4.4, driven by a high brightness 250 pC electron beam with a final energy of 6 GeV. For the FEL source a Linac plus undulator system has been designed based on the C-band Technology, according to the INFN and EU-Xfel consolidated experience, the results of the beam dynamics studies are described by means of start to end simulations for the nominal case. The 250 pC electron beam has been tracked from the photocathode generation down the Linac exit, resulting in a 5 kA electron bunch with final energy of 6 GeV,
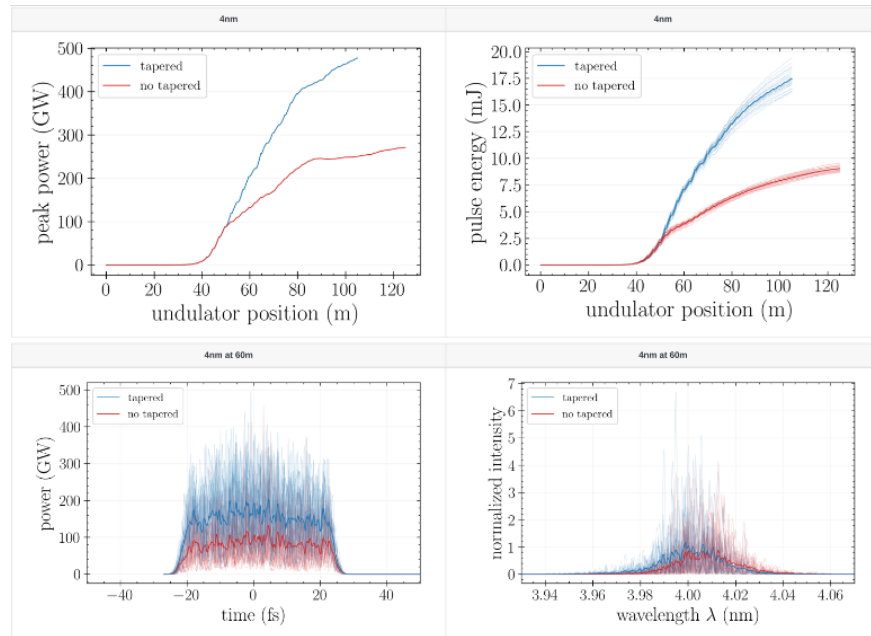
Figure 15: Tapered undulator case: the peak power and pulse energy evolution for the 4nm wavelength show a factor 2 increase with the respect of the untapered case.

energy spread $\sigma_\delta \approx 0.03\,\%$ and $\epsilon_n \approx 0.6\,mm\,mrad$ for the transverse emittance in both planes. A 13 cm period has been chosen for the undulator based on analytical considerations, and simulations have been performed at four different wavelengths to check the flexibility of the undulator design, that results in a mean peak power energy of $100\,GW$ for the wavelengths such as $\lambda_r = 4, 10, 25\,nm$, with an overall length of $\approx 50\,m$, while to reach $\lambda_r = 1\,nm$ a longer setup is needed.

References

[1] T. V. Bondarenko, E. S. Masunov, and S. M. Polozov. BEAMDULAC-BL code for 3D simulation of electron beam dynamics taking into account beam loading and Coulomb field. *Prob. Atomic Sci. Technol.*, 2013(6):114–118, 2013.

[2] Ilya Ashanin, Yulia Kliuchevskaia, Sergey Polozov, and Alexey Pronikov. Beam Dynamics Simulation in a Linear Electron Accelerator - Injector for the 4th Generation Specialized Synchrotron Radiation Source USSR. In *27th Russian Particle Accelerator Conference*, 10 2021.

[3] Sergey Polozov, Ilya Ashanin, Yulia Kliuchevskaia, Michael Lalayan, Alexey Pronikov, and Vladimir Rashchikov. Beam Dynamics Simulation Results in the 6 GeV Top-Up Injection Linac of the 4th Generation Light Source USSR. In *26th Russian Particle Accelerator Conference*, page WEPSB05, 2018.

[4] S. Di Mitri, A. Latina, M. Aicheler, A. Aksoy, D. Alesini, G. Burt, A. Castilla, J. Clarke, H.M.C. Cortés, M. Croia, G. D'Auria, M. Diomede, D. Dunning, M. Ferrario, A. Gallo, A. Giribono, V. Goryashko, A. Mostacci, F. Nguyen, R. Rochow, J. Scifo, B. Spataro, N. Thompson, C. Vaccarezza, A. Vannozzi, X. Wu, and W. Wuensch. Scaling of Beam Collective Effects with Bunch Charge in the CompactLight Free-Electron Laser. *Photonics*, 7(4):125, 2020.

[5] Gerardo D'Auria et al. Status of the CompactLight Design Study. In *39th International Free Electron Laser Conference*, page THP078, 2019.

[6] Anna Giribono et al. Effects of Mode Launcher on Beam Dynamics in Next Generation High Brightness C-Band Guns. *JACoW*, IPAC2021:MOPAB257, 2021.

[7] A. Giribono, A. Bacci, E. Chiadroni, A. Cianchi, M. Croia, M. Ferrario, A. Marocchino, V. Petrillo, R. Pompili, S. Romeo, M. Rossetti Conti, A.R. Rossi, and C. Vaccarezza. Eupraxia@sparc_lab: The high-brightness rf photo-injector layout proposal. *Nuclear Instruments and Methods in Physics Research Section A: Accelerators, Spectrometers, Detectors and Associated Equipment*, 909:282–285, 2018. 3rd European Advanced Accelerator Concepts workshop (EAAC2017).

[8] M. Ferrario, D. Alesini, M.P. Anania, M. Artioli, A. Bacci, S. Bartocci, R. Bedogni, M. Bellaveglia, A. Biagioni, F. Bisesto, F. Brandi, E. Brente-gani, F. Broggi, B. Buonomo, P.L. Campana, G. Campogiani, C. Cannaos, S. Cantarella, F. Cardelli, M. Carpanese, M. Castellano, G. Castorina, N. Catalan Lasheras, E. Chiadroni, A. Cianchi, R. Cimino, F. Ciocci, D. Cirrincione, G.A.P. Cirrone, R. Clementi, M. Coreno, R. Corsini, M. Croia, A. Curcio, G. Costa, C. Curatolo, G. Cuttone, S. Dabagov, G. Dattoli, G. D'Auria, I. Debrot, M. Diomede, A. Drago, D. Di Giovenale, S. Di Mitri, G. Di Pirro, A. Esposito, M. Faiferri, L. Ficcadenti, F. Filippi, O. Frasciello, A. Gallo, A. Ghigo, L. Giannessi, A. Giribono, L. Gizzi, A. Grudiev, S. Guiducci, P. Koester, S. Incremona, F. Iungo, L. Labate, A. Latina, S. Licciardi, V. Lollo, S. Lupi, R. Manca, A. Marcelli, M. Marini, A. Marocchino, M. Marongiu, V. Martinelli, C. Masciovecchio, C. Mastino, A. Michelotti, C. Milardi, V. Minicozzi, F. Mira, S. Morante, A. Mostacci, F. Nguyen, S. Pagnutti, L. Pellegrino, A. Petralia, V. Petrillo, L. Piersanti, S. Pioli, D. Polese, R. Pompili, F. Pusceddu, A. Ricci, R. Ricci, R. Rochow, S. Romeo, J.B. Rosenzweig, M. Rossetti Conti, A.R. Rossi, U. Rotundo, L. Sabbatini, E. Sabia, O. Sans Plannell, D. Schulte, J. Scifo, V. Scuderi, L. Serafini, B. Spataro, A. Stecchi, A. Stella, V. Shpakov, F. Stellato, E. Turco, C. Vaccarezza, A. Vacchi, A. Vannozzi, A. Variola, S. Vescovi, F. Villa, W. Wuen-sch, A. Zigler, and M. Zobov. Eupraxia@sparc_lab design study towards a compact fel facility at lnf. *Nuclear Instruments and Methods in Physics Research Section A: Accelerators, Spectrometers, Detectors and Associated Equipment*, 909:134–138, 2018. 3rd European Advanced

Accelerator Concepts workshop (EAAC2017).

[9]   I.FAST - Innovation Fostering in Accelerator Science and Technology (I.FAST).

[10] A. Giribono, D. Alesini, F. Cardelli, G. Di Raddo, L. Faillace, M. Ferrario, A. Gallo, A. Gizzi, S. Lauciani, A. Liedl, L. Pellegrino, L. Piersanti, C. Vaccarezza, A. Vannozzi, J. Scifo, L. Ficcadenti, G. Castorina, G. Pedrocchi, G. J. Silvi, and T. G. Lucas. Dynamics studies of high brightness electron beams in a normal conducting, high repetition rate c-band injector. *Phys. Rev. Accel. Beams*, 26:083402, Aug 2023.

[11] Marco Pedrozzi. SwissFEL Injector Conceptual Design Report. Technical report, PSI, 2010.

[12] Klaus Flöttmann. Astra: A space charge tracking algorithm, 2011.

[13] M Borland. Elegant: A flexible sdds-compliant code for accelerator simulation, 2000.

[14] Luca Serafini and James B. Rosenzweig. Envelope analysis of intense relativistic quasilaminar beams in rf photoinjectors: A theory of emittance compensation. *Physical Review E*, 55(6):7565–7590, 1997.

[15] M. Xie. Exact and variational solutions of 3D eigenmodes in high gain FELs. *Nucl. Instrum. Meth. A*, 445:59–66, 2000.

[16] S. Reiche. GENESIS 1.3: A fully 3-D time dependent FEL simulation code. *Nucl. Instrum. Meth. A*, 429:243–248, 1999.